

## PLANCK 2015 CONSTRAINTS ON THE NON-FLAT $\phi$ CDM INFLATION MODEL

JUNPEI Ooba,<sup>1,\*</sup> BHARAT RATRA,<sup>2</sup> AND NAOSHI SUGIYAMA<sup>1,3,4</sup>

<sup>1</sup>*Department of Physics and Astrophysics, Nagoya University, Nagoya 464-8602, Japan*

<sup>2</sup>*Department of Physics, Kansas State University, 116 Cardwell Hall, Manhattan, KS 66506, USA*

<sup>3</sup>*Kobayashi-Maskawa Institute for the Origin of Particles and the Universe, Nagoya University, Nagoya, 464-8602, Japan*

<sup>4</sup>*Kavli Institute for the Physics and Mathematics of the Universe (Kavli IPMU), The University of Tokyo, Chiba 277-8582, Japan*

(Dated: August 29, 2018)

### ABSTRACT

We perform Markov chain Monte Carlo analyses to put constraints on the non-flat  $\phi$ CDM inflation model using Planck 2015 cosmic microwave background (CMB) anisotropy data and baryon acoustic oscillation distance measurements. The  $\phi$ CDM model is a consistent dynamical dark energy model in which the currently accelerating cosmological expansion is powered by a scalar field  $\phi$  slowly rolling down an inverse power-law potential energy density. We also use a physically consistent power spectrum for energy density inhomogeneities in this non-flat model. We find that, like the closed- $\Lambda$ CDM and closed-XCDM models, the closed- $\phi$ CDM model provides a better fit to the lower multipole region of the CMB temperature anisotropy data compared to that provided by the tilted flat- $\Lambda$ CDM model. Also, like the other closed models, this model reduces the tension between the Planck and the weak lensing  $\sigma_8$  constraints. However, the higher multipole region of the CMB temperature anisotropy data are better fit by the tilted flat- $\Lambda$  model than by the closed models.

*Keywords:* cosmic background radiation — cosmological parameters — large-scale structure of universe  
— inflation — observations

\* ooba.jiunpei@f.mbox.nagoya-u.ac.jp

## 1. INTRODUCTION

The standard cosmological model, spatially-flat  $\Lambda$ CDM (Peebles 1984), is described by six cosmological parameters:  $\Omega_b h^2$  and  $\Omega_c h^2$ , the current values of the baryonic and cold dark matter (CDM) density parameters multiplied by the square of the Hubble constant  $H_0$  (in units of  $100 \text{ km s}^{-1} \text{ Mpc}^{-1}$ );  $\theta$ , the angular diameter distance as a multiple of the sound horizon at recombination;  $\tau$ , the reionization optical depth; and  $A_s$  and  $n_s$ , the amplitude and spectral index of the (assumed) power-law primordial scalar energy density inhomogeneity power spectrum, (Planck Collaboration 2016a). In this model, the currently accelerated cosmological expansion is powered by the cosmological constant  $\Lambda$ , which is equivalent to a dark energy ideal fluid with equation of state parameter  $w_0 = -1$ . This model assumes flat spatial hypersurfaces, which is largely consistent with most available observational constraints (Planck Collaboration 2016a, and references therein).

However, using a physically consistent non-flat inflation model power spectrum of energy density inhomogeneities (Ratra & Peebles 1995; Ratra 2017), we recently found that cosmic microwave background (CMB) anisotropy measurements do not require flat spatial hypersurfaces in the six parameter non-flat  $\Lambda$ CDM model<sup>1</sup> (Ooba et al. 2018a; Park & Ratra 2018a,b) and also in the seven parameter XCDM model (Ooba et al. 2017; Park & Ratra 2018b), in which the equation of state relating the pressure and energy density of the dark energy fluid is written as  $p_X = w_0 \rho_X$  and  $w_0$  is the additional, seventh, parameter.<sup>2</sup> Also, there are suggestions that flat- $\Lambda$ CDM might not be as compatible with more recent, larger compilations of measurements (Solà et al. 2017a,b, 2018, 2017c; Zhang et al. 2017) that might be more consistent with dynamical dark energy models. These include the simplest, physically consistent, seven parameter spatially-flat  $\phi$ CDM model in which a scalar field  $\phi$  with potential energy density  $V(\phi) \propto \phi^{-\alpha}$  is the dynamical dark energy (Peebles & Ratra 1988; Ratra & Peebles 1988) and  $\alpha > 0$  is the seventh parameter that governs dark energy evolution.<sup>3</sup>

Non-zero spatial curvature brings in a new length scale, in addition to the Hubble scale. Consequently, in non-flat models it is incorrect to assume a power law spectrum for energy density inhomogeneities. Instead in the non-flat case one must use an inflation model to compute a consistent power spectrum. For open spatial hypersurfaces the Gott (1982) open-bubble inflation model is taken as the initial epoch of the cosmological model and one computes zero-point quantum fluctuations during the open inflation epoch and propagates these to the current open accelerating universe where they are energy density inhomogeneities with a power spectrum that is not a power law (Ratra & Peebles 1994, 1995).<sup>4</sup> For closed spatial hypersurfaces Hawking's prescription for the quantum state of the universe (Hawking 1984) can be used to construct a closed inflation model (Ratra 1985, 2017). Zero-point quantum-mechanical fluctuations during closed inflation provide a late-time energy density inhomogeneity power spectrum that is not a power law (Ratra 2017); it is a generalization to the closed case (White & Scott 1996; Starobinsky 1996; Zaldarriaga et al. 1998; Lewis et al. 2000; Lesgourgues & Tram 2014) of the flat-space scale-invariant spectrum.

Compared to the six parameter flat- $\Lambda$ CDM inflation model discussed above, in the non-flat case there is no simple tilt option, so  $n_s$  is no longer a free parameter and is replaced by  $\Omega_k$  which results in the six parameter non-flat  $\Lambda$ CDM model (Ooba et al. 2018a) or the seven parameter non-flat XCDM model (Ooba et al. 2017). Here, we use a physically consistent non-flat seven parameter  $\phi$ CDM scalar field dynamical dark energy model (Pavlov et al. 2013), again with  $n_s$  replaced by  $\Omega_k$ .<sup>5</sup> In this paper we use the Planck 2015 CMB anisotropy data to constrain this seven parameter non-flat  $\phi$ CDM inflation model. We find in this model that the Planck 2015 CMB anisotropy data in conjunction with baryon acoustic oscillation (BAO) measurements do not require that spatial hypersurfaces be flat. The data favor a mildly closed model. These results are consistent with those from our earlier analyses of the six parameter non-flat  $\Lambda$ CDM inflation model (Ooba et al. 2018a) and the seven parameter non-flat XCDM inflation model (Ooba et al. 2017).

The structure of our paper is as follows. In Sec. II we summarize the methods we use in our analyses here. Our parameter constraints are tabulated, plotted, and discussed in Sec. III, where we also attempt to judge how well the best-fit closed- $\phi$ CDM model fits the data. We conclude in Sec. IV.

<sup>1</sup> Here, compared to the flat- $\Lambda$ CDM model,  $n_s$  is replaced by the current value of the spatial curvature density parameter  $\Omega_k$ .

<sup>2</sup> Again,  $n_s$  is replaced by  $\Omega_k$ .

<sup>3</sup> While XCDM is often used to model dynamical dark energy, it is not a physically consistent model as it cannot describe the evolution of energy density inhomogeneities. Also, XCDM does not accurately model  $\phi$ CDM dark energy dynamics (Podariu & Ratra 2001).

<sup>4</sup> For discussions of observational consequences of the open inflation model see Kamionkowski et al. (1994), Górski et al. (1995), Górski et al. (1998), and references therein.

<sup>5</sup> We study the seven parameter flat  $\phi$ CDM model elsewhere (Ooba et al. 2018b).

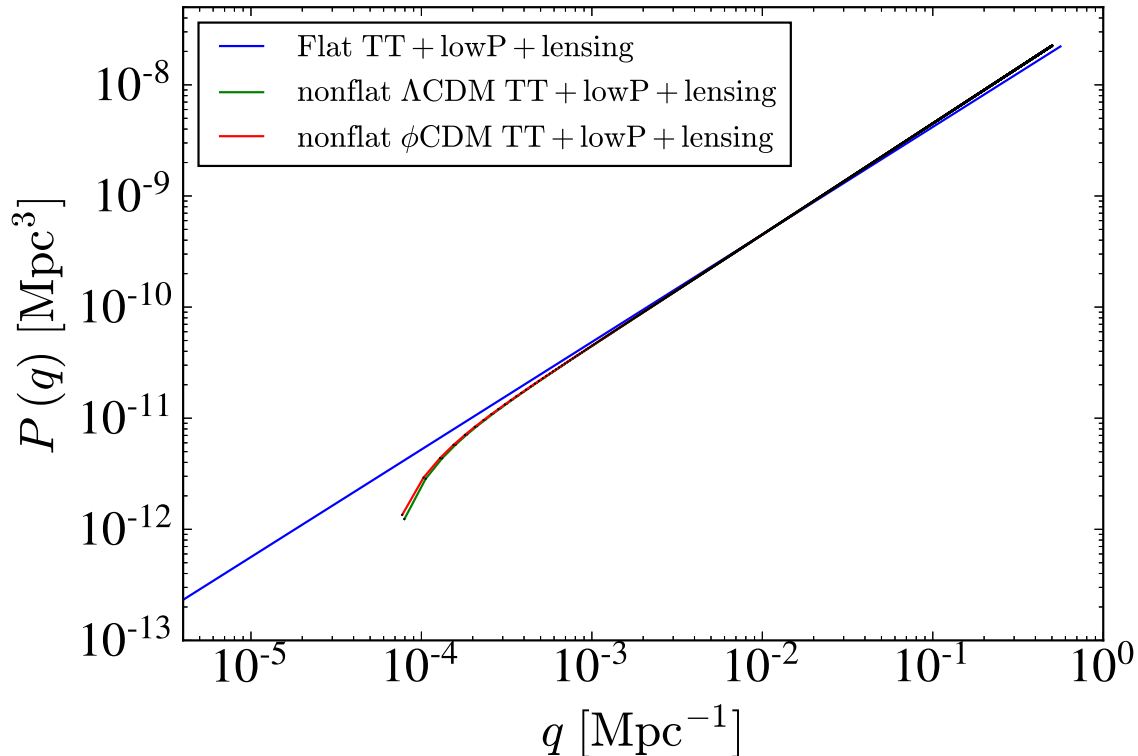


**Figure 1.** Best-fit (see text) gauge-invariant fractional energy density inhomogeneity power spectra. The blue line corresponds to the tilted flat- $\Lambda$ CDM model of [Planck Collaboration \(2016a\)](#). In the closed case, wavenumber  $q \propto A + 1$  where the eigenvalue of the spatial Laplacian is  $-A(A + 2)$ ,  $A$  is a non-negative integer, with  $A = 0$  corresponding to the constant zero-mode on the three sphere, the power spectrum vanishes at  $A = 1$ , and the points on the red and green curves correspond to  $A = 2, 3, 4, \dots$ , see eqns. (8) and (203) of [Ratra \(2017\)](#). On large scales the power spectra for the best-fit closed  $\phi$ CDM (red curve) and closed  $\Lambda$ CDM (green curve) models are suppressed relative to that of the best-fit tilted flat- $\Lambda$ CDM model.  $P(q)$  is normalized by the best-fit value of  $A_s$  at the pivot scale  $k_0 = 0.05$  [ $\text{Mpc}^{-1}$ ].

## 2. METHODS

The equations of motion of the non-flat  $\phi$ CDM model ([Pavlov et al. 2013](#)) are

$$\ddot{\phi} + 3\frac{\dot{a}}{a}\dot{\phi} - \kappa\alpha m_p^2\phi^{-(\alpha+1)} = 0, \quad (1)$$

$$\left(\frac{\dot{a}}{a}\right)^2 = \frac{8\pi}{3m_p^2}(\rho + \rho_\phi) - \frac{k}{a^2}, \quad (2)$$

$$\rho_\phi = \frac{m_p^2}{32\pi} \left( \dot{\phi}^2 + 2\kappa m_p^2 \phi^{-\alpha} \right). \quad (3)$$

Here  $\phi$  is the dark energy scalar field with potential energy density  $V(\phi) = \kappa m_p^2 \phi^{-\alpha}$ ,  $\alpha > 0$ ,  $m_p$  is the Planck mass, and the parameter  $\kappa$  is determined in terms of the other parameters. Also,  $a$  is the scale factor,  $k$  is the curvature parameter that takes values  $-1, 0, 1$ , an overdot denotes a time derivative,  $\rho$  is the energy density of baryonic and cold matter as well as radiation and neutrinos, and  $\rho_\phi$  that of the scalar field. The  $\phi$ CDM model equations of motion has a time-dependent attractor or tracker solution ([Peebles & Ratra 1988](#); [Ratra & Peebles 1988](#); [Pavlov et al. 2013](#)).

We use the open and closed inflation model quantum energy density inhomogeneity power spectrum ([Ratra & Peebles 1995](#); [Ratra 2017](#)) in our analyses of the non-flat  $\phi$ CDM model. Figure 1 shows best-fit power spectra for the non-flat  $\phi$ CDM and non-flat  $\Lambda$ CDM inflation models as well as a tilted flat- $\Lambda$ CDM inflation model power spectrum. In this study we compute the angular power spectra of the CMB anisotropy by using CLASS ([Blas et al. 2011](#))<sup>6</sup> and perform the Markov chain Monte Carlo analyses with Monte Python ([Audren et al. 2013](#)).

<sup>6</sup> Our flat space  $\phi$ CDM CMB anisotropy angular power spectra differ somewhat from earlier results in [Brax et al. \(2000\)](#) and [Mukherjee et al. \(2003\)](#). We have verified that our results are accurate.

The ranges of the cosmological parameters we consider are

$$\begin{aligned} 100\theta &\in (0.5, 10), \quad \Omega_b h^2 \in (0.005, 0.04), \quad \Omega_c h^2 \in (0.01, 0.5), \\ \tau &\in (0.005, 0.5), \quad \ln(10^{10} A_s) \in (0.5, 10), \quad \Omega_k \in (-0.5, 0.5), \quad \alpha \in (0, 8). \end{aligned} \quad (4)$$

The CMB temperature and the effective number of neutrinos were set to  $T_{\text{CMB}} = 2.7255$  K from COBE (Fixsen 2009) and  $N_{\text{eff}} = 3.046$  with one massive (0.06 eV) and two massless neutrino species in a normal hierarchy. The primordial helium fraction  $Y_{\text{He}}$  is inferred from standard Big Bang nucleosynthesis, as a function of the baryon density.

We constrain model parameters by comparing our results to the CMB angular power spectrum data from the Planck 2015 mission (Planck Collaboration 2016a) and the BAO measurements from the matter power spectra obtained by the 6dF Galaxy Survey (6dFGS) (Beutler et al. 2011), the Baryon Oscillation Spectroscopic Survey (BOSS; LOWZ and CMASS) (Anderson et al. 2014), and the Sloan Digital Sky Survey (SDSS) main galaxy sample (MGS) (Ross et al. 2015).

### 3. RESULTS

In this section we tabulate, plot, and discuss the resulting constraints on the seven parameter non-flat  $\phi$ CDM inflation model. Table 1 lists mean values and 68.27% limits on the cosmological parameters (95.45% upper limits on  $\alpha$ ), and Fig. 2 shows two-dimensional constraint contours and one-dimensional likelihoods from the 4 different CMB and BAO data sets used in this study. Here all other parameters are marginalized. We set an additional prior on the Hubble constant,  $h \geq 0.45$ , for the CMB data only cases to realize convergence in a reasonable amount of time.<sup>7</sup> CMB temperature anisotropy spectra for the best-fit non-flat  $\phi$ CDM models are shown in Fig. 3, compared with non-flat and tilted spatially-flat  $\Lambda$ CDM models. Contours at 68.27% and 95.45% confidence level in the  $\sigma_8$ - $\Omega_m$  plane are shown in Fig. 4 with other parameters marginalized.

**Table 1.** 68.27% (or 95.45% on  $\alpha$ ) confidence limits on cosmological parameters of the non-flat  $\phi$ CDM model from CMB and BAO data.

Parameter	TT+lowP ( $h \geq 0.45$ )	TT+lowP+lensing ( $h \geq 0.45$ )	TT+lowP+BAO	TT+lowP+lensing+BAO
$\Omega_b h^2$	$0.02326 \pm 0.00022$	$0.02303 \pm 0.00020$	$0.02303 \pm 0.00020$	$0.02300 \pm 0.00020$
$\Omega_c h^2$	$0.1094 \pm 0.0011$	$0.1091 \pm 0.0011$	$0.1095 \pm 0.0011$	$0.1095 \pm 0.0011$
$100\theta$	$1.04296 \pm 0.00041$	$1.04303 \pm 0.00041$	$1.04293 \pm 0.00041$	$1.04298 \pm 0.00041$
$\tau$	$0.110 \pm 0.020$	$0.104 \pm 0.021$	$0.137 \pm 0.018$	$0.129 \pm 0.013$
$\ln(10^{10} A_s)$	$3.130 \pm 0.041$	$3.116 \pm 0.042$	$3.183 \pm 0.036$	$3.168 \pm 0.026$
$\Omega_k$	$-0.073 \pm 0.017$	$-0.034 \pm 0.016$	$-0.006 \pm 0.003$	$-0.006 \pm 0.003$
$\alpha$ [ $2\sigma$ limit]	$< 1.82$	$< 3.26$	$< 0.305$	$< 0.304$
$H_0$ [km/s/Mpc]	$48.76 \pm 2.39$	$54.70 \pm 6.86$	$69.13 \pm 1.06$	$67.09 \pm 1.11$
$\Omega_m$	$0.56 \pm 0.06$	$0.46 \pm 0.12$	$0.29 \pm 0.01$	$0.29 \pm 0.01$
$\sigma_8$	$0.735 \pm 0.031$	$0.716 \pm 0.053$	$0.815 \pm 0.021$	$0.806 \pm 0.014$

We find that the 95.45% limits of the spatial curvature density parameter are

$$\Omega_k = -0.034^{+0.028}_{-0.033} \quad (95.45\%, \text{ TT + lowP + lensing}), \quad (5)$$

$$\Omega_k = -0.006 \pm 0.005 \quad (95.45\%, \text{ TT + lowP + lensing + BAO}). \quad (6)$$

Both data sets result in best-fit models about  $3\sigma$  away from flat. We note that many analyses based on a variety of different, non-CMB, observations also do not rule out non-flat dark energy models (Farooq et al. 2015; Sapone et al. 2014; Li et al. 2014; Cai et al. 2016; Chen et al. 2016; Yu & Wang 2016; L’Huillier & Shafieloo 2017; Farooq et al. 2017; Li et al. 2016; Wei & Wu 2017; Rana et al. 2017; Yu et al. 2018; Mitra et al. 2018; Ryan et al. 2018).

<sup>7</sup> We thank C.-G. Park for discussions about this and for pointing out a numerical error in our initial analyses. Our corrected results here are in very good agreement with those of Park & Ratra (2018c).

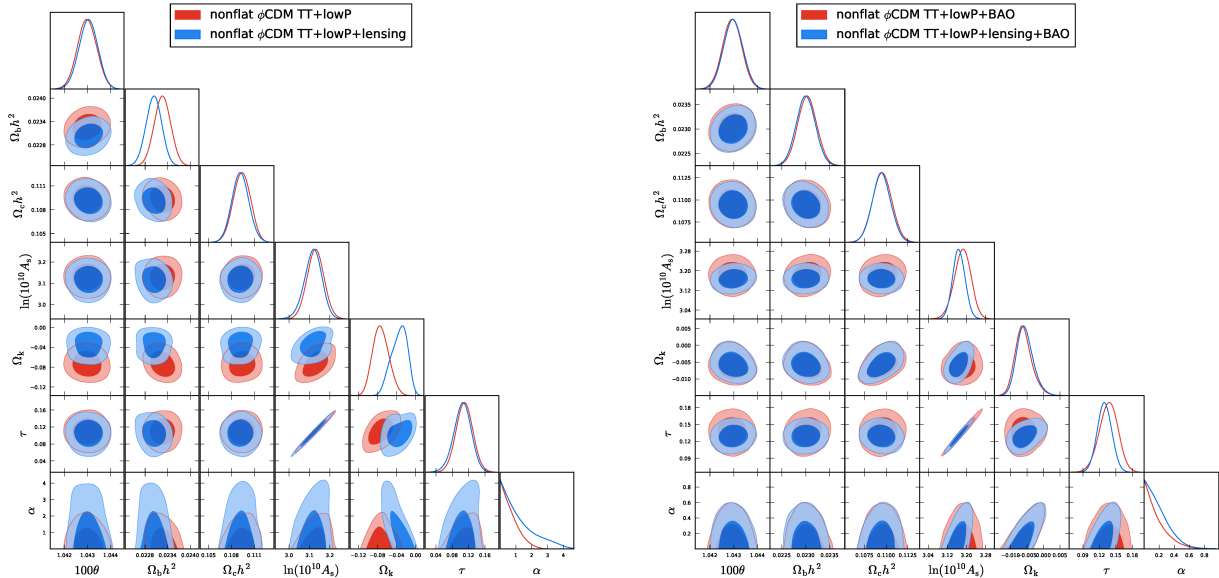


**Figure 2.** 68.27% and 95.45% confidence level contours for the non-flat  $\phi$ CDM inflation model using various data sets, with the other parameters marginalized.

From the TT + lowP + lensing + BAO column in Table 1, we see that  $H_0 = 67.09 \pm 1.11 \text{ km s}^{-1} \text{ Mpc}^{-1}$ . This is consistent with most other determinations (Chen & Ratra 2011; Calabrese et al. 2012; Sievers et al. 2013; Aubourg et al. 2015; L’Huillier & Shafieloo 2017; Luković et al. 2016; Chen et al. 2017; Wang et al. 2017; Lin & Ishak 2017; Abbott et al. 2017; Yu et al. 2018), but a little lower than local determinations (Freedman et al. 2012; Riess et al. 2016). The  $\Omega_m$  result is also consistent with most other determinations (e.g., Chen & Ratra 2003).

All three closed inflation models are more consistent with the low- $\ell$   $C_\ell$  observations<sup>8</sup> and the weak lensing  $\sigma_8$  constraints than is the best fit spatially-flat tilted  $\Lambda$ CDM, but they do worse at fitting the higher- $\ell$   $C_\ell$  measurements.

**Table 2.** Minimum  $\chi_{\text{eff}}^2$  values for the best-fit closed- $\phi$ CDM (and tilted flat- $\Lambda$ CDM) inflation model.

Data sets	$\chi_{\text{eff}}^2$	d.o.f.
TT+lowP ( $h \geq 0.45$ )	11272 (11262)	188 (189)
TT+lowP+lensing ( $h \geq 0.45$ )	11294 (11272)	196 (197)
TT+lowP+BAO	11287 (11266)	192 (193)
TT+lowP+lensing+BAO	11298 (11277)	200 (201)

<sup>8</sup> At low  $\ell$ , polarization anisotropy systematics (and possibly foreground contamination) are more significant, as is cosmic variance. Our analyses here assume that the low- $\ell$  error bars account for all relevant effects.

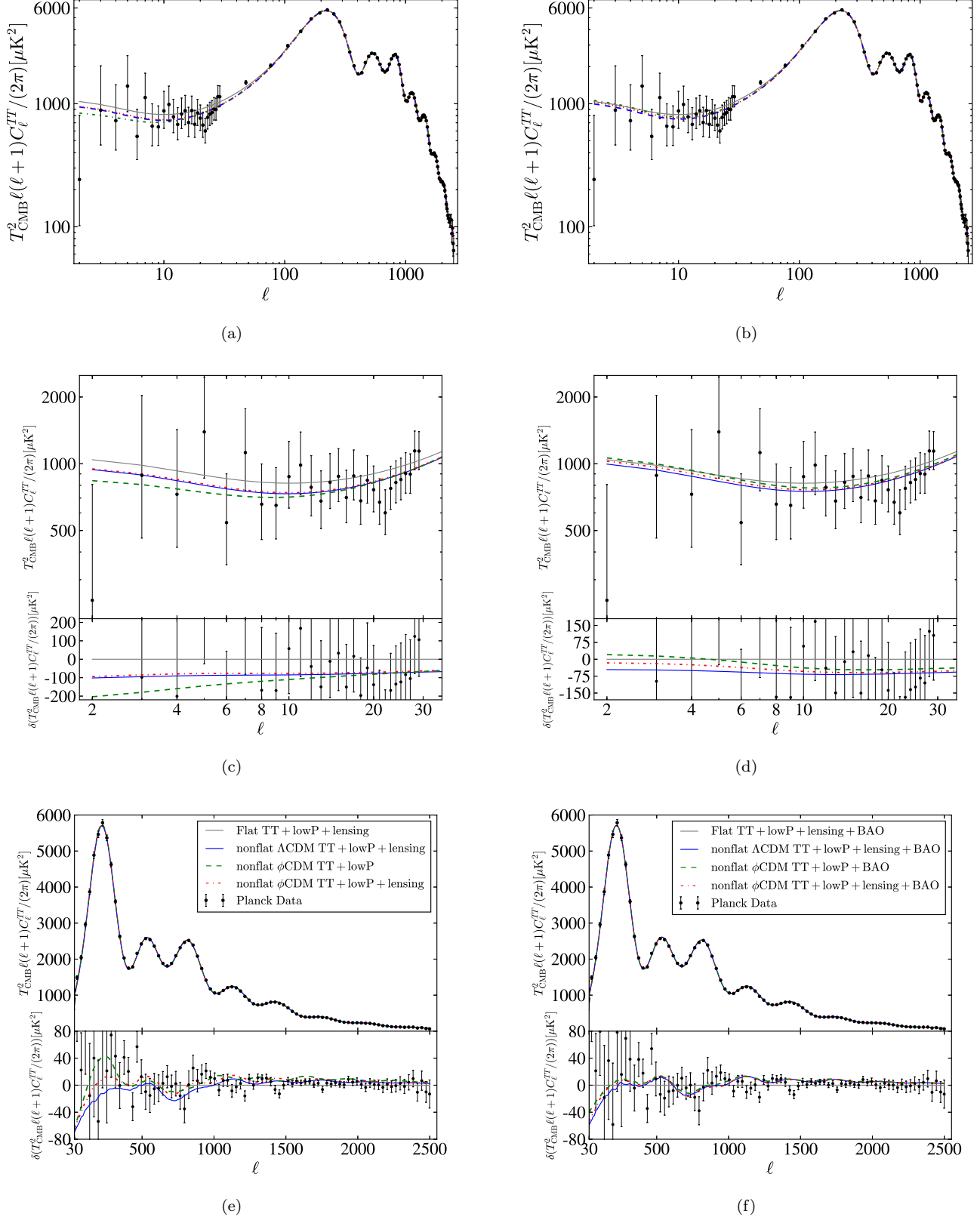


**Figure 3.** The  $C_\ell$  for the best-fit non-flat  $\phi\text{CDM}$ , non-flat  $\Lambda\text{CDM}$  and spatially-flat tilted  $\Lambda\text{CDM}$  (gray solid line) models. Linestyle information are in the boxes in the two lowest panels. Planck 2015 data are shown as black points with error bars. Left panels (a), (c) and (e) are from CMB data alone analyses, while right panels (b), (d) and (f) analyses also include BAO data. The top panels show the all- $\ell$  region. The middle panels show the low- $\ell$  region  $C_\ell$  and residuals. The bottom panels show the high- $\ell$  region  $C_\ell$  and residuals.

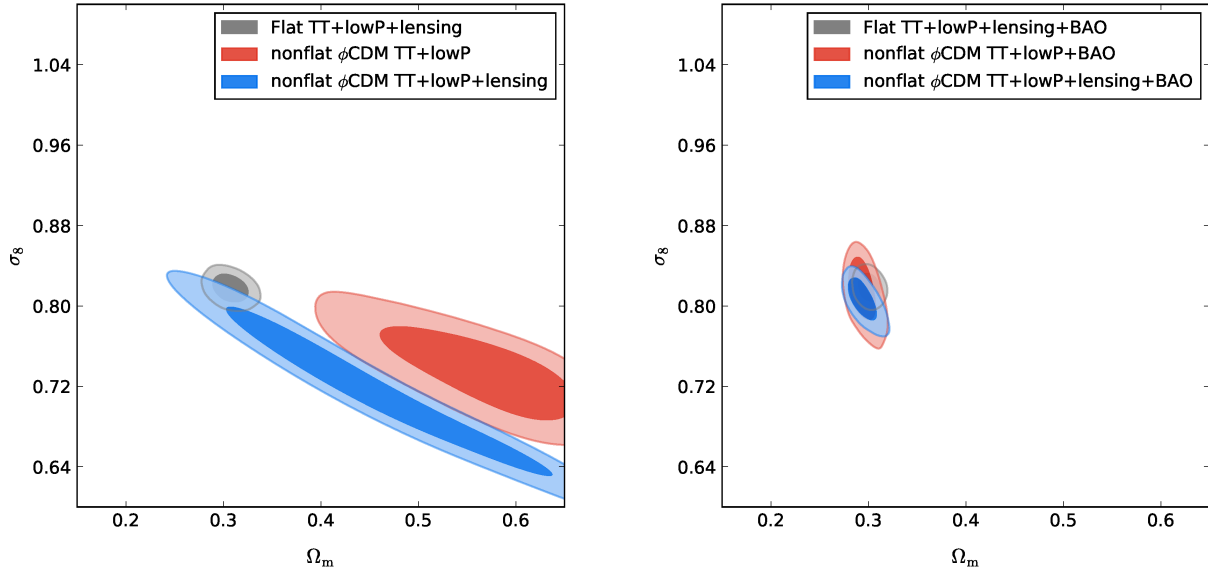


**Figure 4.** 68.27% and 95.45% confidence level contours in the  $\sigma_8$ - $\Omega_m$  plane.

**Table 3.**  $\chi^2$  values for the best-fit closed- $\phi$ CDM (and tilted flat- $\Lambda$ CDM) inflation model.

Data	TT+lowP ( $h \geq 0.45$ )	TT+lowP+lensing ( $h \geq 0.45$ )	TT+lowP+BAO	TT+lowP+lensing+BAO
CMB low- $\ell$	134.63 (129.83)	126.26 (126.06)	155.12 (130.06)	135.69 (126.00)
CMB high- $\ell$	151.18 (77.13)	135.81 (82.46)	134.19 (73.64)	127.58 (80.82)
CMB all- $\ell$	285.81 (206.97)	271.84 (218.43)	293.16 (207.73)	276.16 (220.31)
CMB lensing	—	9.77 (9.90)	—	10.04 (9.92)
BAO	—	—	3.85(4.03)	2.85 (3.58)
d.o.f.	188 (189)	196 (197)	192 (193)	200 (201)

It is important to quantitatively understand how well the best-fit closed- $\phi$ CDM inflation model does relative to the best-fit tilted flat- $\Lambda$ CDM model in fitting the data. As for the closed- $\Lambda$ CDM and closed-XCDM cases (Ooba et al. 2018a, 2017), we are unable to resolve this in a quantitative manner, although qualitatively, overall, the best-fit closed- $\phi$ CDM model does not do as well as the best-fit tilted flat- $\Lambda$ CDM model. However, for some data it does better than the best-fit closed- $\Lambda$ CDM inflation model (Ooba et al. 2018a), which has one fewer parameter, as well as better than the best-fit closed-XCDM case (Ooba et al. 2017) which has the same number of parameters.

Table 2 lists the minimum  $\chi_{\text{eff}}^2 = -2\ln(L_{\text{max}})$  determined from the maximum value of the likelihood, for the four data sets we study, for both the closed- $\phi$ CDM and tilted flat- $\Lambda$ CDM inflation models, as well as the number of (binned data) degrees of freedom (d.o.f.). The d.o.f. are determined from combinations of 112 low- $\ell$  TT + lowP, 83 high- $\ell$  TT, 8 lensing CMB (binned) measurements, 4 BAO measurements, and 7 (or 6 for the tilted flat- $\Lambda$ CDM) model parameters. Almost certainly the large  $\chi_{\text{eff}}^2$  values are the result of the many nuisance parameters that have been marginalized over, as the tilted flat- $\Lambda$ CDM model is said to be a good fit to the data. From this table we see that  $\Delta\chi_{\text{eff}}^2 = 22(21)$  for the closed- $\phi$ CDM inflation model (196 (200) d.o.f.), relative to the tilted flat- $\Lambda$ CDM case (197 (201) d.o.f.), for the TT + low P + lensing (+ BAO) data combination.<sup>9</sup> While this might make the closed- $\phi$ CDM model much less probable, one can see from the residual panels of Fig. 3 (e) & (f) that this  $\Delta\chi_{\text{eff}}^2$  is apparently caused by many small deviations, and not by a few significant outliers. This allows for the possibility that a slight increase in the error bars or a mild non-Gaussianity in the errors could raise the model probabilities.

<sup>9</sup> When closed- $\phi$ CDM is compared to both closed- $\Lambda$ CDM and closed-XCDM,  $\Delta\chi_{\text{eff}}^2 = 2(0)$ , for these two data sets, where closed- $\Lambda$ CDM has the same d.o.f. as flat- $\Lambda$ CDM and closed-XCDM the same as closed- $\phi$ CDM (Ooba et al. 2018a, 2017).

While there are correlations in the data, it is also instructive to consider a standard goodness of fit  $\chi^2$  that only makes use of the diagonal elements of the correlation matrix. These are listed in Table 3 for the four data sets we study and for both the closed- $\phi$ CDM and tilted flat- $\Lambda$ CDM inflation models. From Table 3 for the TT + low P + lensing data, we see that the  $\chi^2$  per d.o.f. is 282/196 (228/197, 268/197, 273/196) for the closed- $\phi$ CDM (tilted flat- $\Lambda$ CDM, closed- $\Lambda$ CDM, closed-XCDM) inflation model, and when BAO data is added to the mix these become 289/200 (234/201, 293/201, 294/200). Again, while the closed- $\phi$ CDM model is less favored than the tilted flat- $\Lambda$ CDM case (and is the most favored of the closed models we study for the +BAO data combination), it is not straightforward to assess the quantitative significance of this. In addition to the points mentioned at the end of the previous paragraph, here we also ignore all the off-diagonal information in the correlation matrix, so it is meaningless to compute standard probabilities from such  $\chi^2$ 's. All in all, while the best-fit closed- $\phi$ CDM inflation model appears less favored, it might be useful to perform a more thorough analysis of the model.<sup>10</sup>

#### 4. CONCLUSION

We have constrained the physically consistent seven parameter non-flat  $\phi$ CDM inflation model using Planck 2015 CMB data and BAO distance measurements.

Unlike the results of the seven parameter non-flat tilted  $\Lambda$ CDM model in Planck Collaboration (2016a), our seven parameter non-flat  $\phi$ CDM inflation model is not forced to be flat even when the BAO data are added to the mix. This is also the case for the non-flat  $\Lambda$ CDM and non-flat XCDM models we studied earlier (Ooba et al. 2018a, 2017; Park & Ratra 2018a,b). We find that  $\Omega_k = -0.006 \pm 0.005$  at  $2\sigma$  and that the best-fit point is about  $3\sigma$  away from flat. In this case the improved agreement with the low- $\ell$   $C_\ell$  observations<sup>11</sup> and the weak lensing  $\sigma_8$  are not as good compared with the results from the analyses using only the Planck 2015 CMB data. However, the BAO and CMB data are from very disparate redshifts and it is possible that a better model for the intervening epoch or an improved understanding of one or both sets of measurements might alter this conclusion.

A more thorough analysis of the non-flat  $\Lambda$ CDM, XCDM, and  $\phi$ CDM inflation models is needed<sup>12</sup> to establish if one of them is viable and can help resolve some of the low- $\ell$   $C_\ell$  issues as well as possibly the  $\sigma_8$  power issues, without significantly worsening the fit to the higher- $\ell$   $C_\ell$ 's. Perhaps non-zero spatial curvature might be more important for this purpose than is dark energy dynamics.

#### ACKNOWLEDGMENTS

This work is supported by Grants-in-Aid for Scientific Research from JSPS (Nos. 16J05446 (J.O.) and 15H05890 (N.S.)). B.R. is supported in part by DOE grant DE-SC0011840.

<sup>10</sup> It has previously been noted that the constraints derived from higher- $\ell$  and lower- $\ell$  Planck 2015 CMB anisotropy data differ slightly (Addison et al. 2016; Planck Collaboration 2016b). It might be useful to revisit this issue using the non-flat models we have studied, to see if this makes a difference.

<sup>11</sup> As noted above, systematics, foreground contamination, and cosmic variance play a bigger roll at lower  $\ell$  and we assume that the data error bars correctly account for all effects.

<sup>12</sup> As part of such an analysis, it would be useful to examine smaller-scale predictions of these models, as well as potential CMB spectral distortions (for a review of spectral distortions see Chluba 2018). We note that when fit to the Planck 2015 data non-flat inflation models have a significantly higher reionization optical depth with interesting implications for reionization models (Mitra et al. 2018).



## REFERENCES

- Abbott, T. M. C. et al. 2017, arXiv:1711.00403
- Addison, G. E., et al. 2016, *ApJ*, 818, 132 [arXiv:1511.00055]
- Anderson, L. et al. 2014, *MNRAS*, 441, 24 [arXiv:1312.4877]
- Aubourg, E. et al. 2015, *Phys. Rev. D*, 92, 123516 [arXiv:1411.1074]
- Audren, B., Lesgourgues, J., Benabed, K., & Prunet, S. 2013, *JCAP*, 1302, 001 [arXiv:1210.7183]
- Beutler, F. et al. 2011, *MNRAS*, 416, 3017 [arXiv:1106.3366]
- Blas, D., Lesgourgues, J., & Tram, T. 2011, *JCAP*, 1107, 034 [arXiv:1104.2933]
- Brax, P., Martin, J., & Riazuelo, A. 2000, *Phys. Rev. D*, 62, 103505 [arXiv:astro-ph/0005428]
- Cai, R.-G., Guo, Z.-K., & Yang, T. 2016, *Phys. Rev. D*, 93, 043517 [arXiv:1509.06283]
- Calabrese, E., Archidiacono, M., Melchiorri, A., & Ratra, B. 2012, *Phys. Rev. D*, 86, 043520 [arXiv:1205.6753]
- Chluba, J. 2018, arXiv:1805.02915
- Chen, G., & Ratra, B. 2003, *PASP*, 115, 1143 [arXiv:astro-ph/0302002]
- Chen, G., & Ratra, B. 2011, *PASP*, 123, 1127 [arXiv:1105.5206]
- Chen, Y., Kumar, S., & Ratra, B. 2017, *ApJ*, 835, 86 [arXiv:1606.07316]
- Chen, Y., et al. 2016, *ApJ*, 829, 61 [arXiv:1603.07115]
- Farooq, O., Madiyar, F. R., Crandall, S., & Ratra, B. 2017, *ApJ*, 835, 26 [arXiv:1607.03537]
- Farooq, O., Mania, D., & Ratra, B. 2015, *ApSS*, 357, 11 [arXiv:1308.0834]
- Fixsen, D. J. 2009, *ApJ*, 707, 916 [arXiv:0911.1955]
- Freedman, W. L., et al. 2012, *ApJ*, 758, 24 [arXiv:1208.3281]
- Górski, K. M., et al. 1998, *ApJS*, 114, 1 [arXiv:astro-ph/9608054]
- Górski, K. M., Ratra, B., Sugiyama, N., & Banday, A. J. 1995, *ApJ*, 444, L65 [arXiv:astro-ph/9502034]
- Gott, J. R. 1982, *Nature*, 295, 304
- Hawking, S. W. 1984, *Nucl. Phys. B*, 239, 257
- Kamionkowski, M., Ratra, B., Spergel, D. N., & Sugiyama, N. 1994, *ApJ*, 434, L1 [arXiv:astro-ph/9406069]
- Lesgourgues, J., & Tram, T. 2014, *JCAP*, 1409, 032 [arXiv:1312.2697]
- Lewis, A., Challinor, A., & Lasenby, A. 2000, *ApJ*, 538, 473 [arXiv:astro-ph/9911177]
- L'Huillier, B., & Shafieloo, A. 2017, *JCAP*, 1701, 015 [arXiv:1606.06832]
- Li, Y.-L., Li, S.-Y., Zhang, T.-J., & Li, T.-P. 2014, *ApJ*, 789, L15 [arXiv:1404.0773]
- Li, Z., Wang, G.-J., Liao, K., & Zhu, Z.-H. 2016, *ApJ*, 833, 240 [arXiv:1611.00359]
- Lin, W., & Ishak, M. 2017, arXiv:1708.09813
- Luković, V. V., D'Agostino, R., & Vittorio, N. 2016, *Astron. Astrophys.*, 595, A109 [arXiv:1607.05677]
- Mitra, S., Choudhury, T. R., & Ratra, B. 2018, *MNRAS*, 479, 4566 [arXiv:1712.00018]
- Mukherjee, P., et al. 2003, *ApJ*, 598, 767 [arXiv:astro-ph/0306147]
- Ooba, J., Ratra, B., & Sugiyama, N. 2018, *ApJ*, in press [arXiv:1707.03452]
- Ooba, J., Ratra, B., & Sugiyama, N. 2017, arXiv:1710.03271
- Ooba, J., Ratra, B., & Sugiyama, N. 2018b, arXiv:1802.05571
- Park, C.-G., & Ratra, B. 2018a, arXiv:1801.00213
- Park, C.-G., & Ratra, B. 2018b, arXiv:1803.05522
- Park, C.-G., & Ratra, B. 2018c, arXiv:1807.07421
- Pavlov, A., Westmoreland, S., Saaïdi, K., & Ratra, B. 2013, *Phys. Rev. D*, 88, 123513 [arXiv:1307.7399]
- Peebles, P. J. E. 1984, *ApJ*, 284, 439
- Peebles, P. J. E., & Ratra, B. 1988, *ApJ*, 325, L17
- Planck Collaboration 2016a, *Astron. Astrophys.*, 594, A13 [arXiv:1502.01589]
- Planck Collaboration 2016b, arXiv:1608.02487
- Podariu, S., & Ratra, B. 2001, *ApJ*, 532, 109 [arXiv:astro-ph/9910527]
- Rana, A., Jain, D., Mahajan, S., & Mukherjee, A. 2017, *JCAP*, 1703, 028 [arXiv:1611.07196]
- Ratra, B. 1985, *Phys. Rev. D*, 31, 1931
- Ratra, B. 2017, *Phys. Rev. D*, 96, 103534 [arXiv:1707.03439]
- Ratra, B., & Peebles, P. J. E. 1988, *Phys. Rev. D*, 37, 3406
- Ratra, B., & Peebles, P. J. E. 1994, *ApJ*, 432, L5
- Ratra, B., & Peebles, P. J. E. 1995, *Phys. Rev. D*, 52, 1837
- Riess, A. G., et al. 2016, *ApJ*, 826, 56 [arXiv:1604.01424]
- Ross, A. J. et al. 2015, *MNRAS*, 449, 835 [arXiv:1409.3242]
- Ryan, J., Doshi, S., & Ratra, B. 2018, *MNRAS*, 480, 759 [arXiv:1805.06408]
- Sapone, D., Majerotto, E., & Nesseris, S. 2014, *Phys. Rev. D*, 90, 023012 [arXiv:1402.2236]
- Sievers, J. L., et al. 2013, *JCAP*, 1310, 060 [arXiv:1301.0824]
- Solà, J., de Cruz Pérez, J., & Gómez-Valent, A. 2018, *Europhys. Lett.*, 121, 39001 [arXiv:1606.00450]
- Solà, J., de Cruz Pérez, J. & Gómez-Valent, A. 2017c, arXiv:1703.08218
- Solà, J., Gómez-Valent, A., & de Cruz Pérez, J. 2017a, *ApJ*, 836, 43 [arXiv:1602.02103]
- Solà, J., Gómez-Valent, A., & de Cruz Pérez, J. 2017b, *Mod. Phys. Lett. A*, 32, 1750054 [arXiv:1610.08965]

- Starobinsky, A. A. 1996, arXiv:astro-ph/9603075
- Wang, Y., Xu, L., & Zhao, G.-B. 2017, arXiv:1706.09149
- Wei, J.-J., & Wu, X.-F. 2017, ApJ, 838, 160  
[arXiv:1611.00904]
- White, M., & Scott, D. 1996, ApJ, 459, 415  
[arXiv:astro-ph/9508157]
- Yu, H., Ratra, B., & Wang, F.-Y. 2018, ApJ, 856, 3  
[arXiv:1711.03437]
- Yu, H., & Wang, F. Y. 2016, ApJ, 828, 85  
[arXiv:1605.02483]
- Zaldarriaga, M., Seljak, U., & Bertschinger, E. 1998, ApJ, 494, 491 [arXiv:astro-ph/9704265]
- Zhang, X., et al. 2017, Res. Astron. Astrophys., 17, 6  
[arXiv:1703.08293]